A MATHEMATICAL MODEL FOR AN EXPANDING FOAM

L. W. Schwartz & R. V. Roy

Department of Mechanical Engineering
University of Delaware
Newark, Delaware, USA

June 2002

A theoretical and numerical model is presented for the shape evolution of the thin liquid films separating the gas bubbles in a foam. The motion is due to capillary action, surface tension gradients, and the overall expansion of the foam. The expansion is the result of the increase in gas content with time. Process modeling is accomplished via the solution of three coupled partial differential equations. Two time scales are included in the model: a process time and a drying or curing time. It is demonstrated that the amount of surfactant is the dominant control mechanism for the final film thickness. If sufficient surfactant is present, the films will be shown to dilate uniformly in space. A number of known features of expanding foams are reproduced by the model.

1. Introduction

This paper presents a theoretical and numerical model for predicting the shape evolution of the liquid region in an expanding gas/liquid foam. Results are directly relevant to rapidly-expanding foams that ultimately solidify, such as a polyurethane (PU) foam and other plastic foams. Certain features of the present modeling effort are also applicable to aqueous foams and emulsions, as well as to flocculation of droplets and bubbles.

Foams form an important intermediate class of matter, whereby liquids and gases can be blended together to form a low-density substance that can persist for long times. Foams find application in many industries including foodstuffs, personal care products, petrochemicals and defense. Sometimes the generation and persistance of foams is undesirable; an important example of this is the foaming of lubricating oils.

A two-dimensional geometry and a high degree of symmetry have been assumed in the present model. Because of this, the physics is considerably simplified and only a small portion of the flow, termed a "unit cell," needs to be analyzed. While an actual foam is, of course, three-dimensional, most of the liquid is to be found in the region where three thin liquid films, or lamellae, meet at mutual angles of 120 degrees. These are the so-called *Plateau borders*. The Plateau borders form the cross-sections of the *struts* where much of the liquid accumulates. For industrial foams, the liquid ultimately solidifies so that the struts become structural elements. Thus the problem of predicting the partition of liquid between the films and the Plateau borders is primarily a two-dimensional one. Because the cells are assumed to be small, gravity does not have a significant influence of the flow between the thin films

and the borders. Thus gravity is omitted from the present study. Clearly gravity does cause significant drainage, along the interconnected system of struts, in a non-solidifying aqueous foam or soap froth [1].

The main goal of the present study is to present the form of a *minimal model* for this complicated process. By demonstrating the computability of the model to be presented here, we will have established the basic framework that will allow a quantitative description and a better understanding of a number of industrially important processes. Such a model can be interrogated to predict the overall effects of particular changes in one or more physical input variables. The model developed here can be criticized for its crudeness in certain aspects; some suggestions for improvement will be given in the concluding section.

The flow is driven primarily by a given rate of gas generation or injection; this requires the liquid films between Plateau borders to stretch. At each instant of time the profile shape changes in response to the newly-imposed deformation and the fact that the time-evolving system is not at mechanical equilibrium. The stretching stops after a period of time, called the *process time* by us, corresponding, for example, to the foam mixture filling the available space in a container. However, the film profile continues to evolve, under the action of hydrodynamic forces, until the liquid has solidified.

Physical quantities in the model include viscosity, surface tension, and various parameters associated with the presence of surfactant. In general the effect of surface tension (*capillarity*) is to draw liquid back into the Plateau borders because these borders are highly-curved and thus the (capillary) pressure is lower there than in the thin films. Since the liquid volume is conserved, this backflow thins the films that separate the gas bubbles. In industrial parlance, the thin films are often referred to as *windows*. The numerical solution to the model problem, as formulated here, will demonstrate that, if little or no surfactant is present, windows will become very thin and will break. This breaking may occur either during the expansion or the fully-expanded stages of the motion. Both situations can be observed in real foams.

With increasing amounts of surfactant, the windows will become thicker. We will show that this is due, fundamentally, to a surface-tension-gradient stress (sometimes called a *Marangoni* stress) that stiffens or *hardens* the liquid-gas interface. This stress changes the nature of the backflow and diminishes it very substantially. There is a critical amount of surfactant for which the backflow will be maximally retarded. If this amount is present, the interface will be almost completely hardened. Under these conditions, during the expansion phase, the interface will be shown to dilate uniformly. That is, each element of the interface, or the thin film, will lengthen by the same fractional amount during a given time interval. With this critical surfactant level, an assumed simple Newtonian liquid that is curing uniformly in space will have the thickest possible windows, for a given set of process conditions. Surface hardening in soap films is discussed by Mysels *et al* [2]. The model results to be given in this paper are similar to the experimental observations that they report. In prior work an assumed completely-hardened surface for a foam was used in analytical calculations that led to predictions of foam extensional viscosity, *i. e.* the viscosity of a foam during an imposed purely-extensional motion [3]. We believe that the first numerical demonstration of surface hardening, due to surfactant, was

done by us several years ago for a thin liquid coating on a solid substrate [4].

The mathematical model that we develop here consists of three coupled nonlinear partial differential equations as well as appropriate boundary conditions. The three unknown functions are the film profile, the surfactant distribution, and the interfacial speed distribution. Each of these functions vary in space and time. The model is an adaptation and significant extension of a model developed by us to explain the behavior of draining soap films [5]. For a soap film on a vertical wire frame that is draining under the influence of gravity, it has been observed experimentally that rapid thinning occurs at low surfactant levels while high surfactant concentrations result in thick films that drain quite slowly. In addition, these two regimes have characteristically different profile shapes. All these features, as observed by Mysels [2], were successfully reproduced and explained by the earlier model. In addition, that model reproduced the occurrence of very thin, so called *black*, films that have been observed to appear during late stages of draining. This validation of the basic model, in a related problem, is important since it is unlikely that accurate time-dependent *in-situ* profile measurements can be made within a three-dimensional soap-water foam. It is even less likely that such measurements could be made within expanding industrial foams.

As will be shown below, there are other features that can be included in the theoretical and numerical model that will influence the final shape and thickness of the windows in an expanded foam. The expansion history is an input function that includes the specification of both the average growth speed as well as the form of the speed versus time relationship. The final volume fraction, essentially equivalent to the final density of a dry industrial foam product, can also be varied. A diffusion constant is also specified to model the rate of spontaneous spreading of the surfactant along the interface. Diffusion is a dissipative process and relatively large values of the diffusion constant can be shown to relax surface hardening and ultimately lead to thinner films. The rate of drying/curing is another input variable. This variable determines the elapsed time that is required for the foam matrix material to solidify. The molecular repulsion that leads to stable "black" film that is commonly observed in soap films is also included in the model. This effect, usually termed *disjoining pressure,* is important for films that become exceedingly thin. It is our belief that the primary role played by disjoining pressure is the control of window breakage which it tends to prevent. Thus it is potentially important in modeling the production of flexible foam products where most of the windows will ultimately break. The effect would be much less important for rigid foam products because these are characterized by relatively thick unbroken windows.

This paper also includes some results obtained with the numerical algorithm that has been developed based on the present theory. Certain known features of PU foam Plateau border and window shapes have been reproduced. These include, for example, the observed occurrence of localized thin regions or *dimples* near border-film junctures [6].

The next section demonstrates the reduction in the number of controlling parameters that may be accomplished using dimensional analysis. Sections 3 through 5 specify the forms of input functions that ultimately determine the shape of the final dry film. These include the initial conditions, the function that controls the rate of stretching of the liquid films, and a

viscosity-versus-time law. The system of coupled partial differential equations and the associated boundary conditions are given in section 6. The argument demonstrating that strong surfactant effect will result in spatially uniform stretching of the thin films is given in subsection 6.2. Some sample results, using the numerical model, are given in sections 7 and 8. Section 8 also presents a model for generalized Newtonian rheology of the liquid.

2. Model parameters

Within the present model, a number of parameters influence the final shape of the liquid region. Five parameters are included in the disjoining pressure model. For thick films for which window breaking is not an issue, these parameters will have little or no effect. We will consider the remaining parameters first and discuss the disjoining effect afterward.

Let us assume that we wish to solve for a particular value of the final film thickness, such as the minimum thickness, for example. Alternatively, we could consider some suitably defined average window thickness. Let one of these be denoted as $\bar{h}$. The model assumes that $\bar{h}$ depends on a number of input parameters according to

$$\bar{h} = f\left(\mu_0, \sigma_0, L_0, U_0, F_0, t_{proc}, t_{dry}, K, D_0, n\right) \ . \tag{2.1}$$

Here f denotes some functional dependence. Determination of the actual form of this function is a principal objective of the present work. It will need to be found numerically through solution of the model equations. The parameters on the right of equation (2.1) are:

(i) F_0 is the (essentially arbitrary) initial gas area fraction. The maximum possible value of F_0 is $F^* \approx 0.907$ for an assumed initially circular hexagonal pattern of bubbles. This is the planar close-packing value, *i. e.* the value at which circular bubbles would touch one another. Thus F_0 must be smaller than F^*. Provided the bubbles are not too close to each other, their mutual influence will be small and the circular initial condition can be justified. They will continue to grow as approximate circles until they get close to each other and viscous and other effects become important. However, since the theory we use postulates that the liquid area is long and thin, F_0 must not be too small. Good values for F_0 are in the approximate range (0.5,0.85) Within this range, the actual value of F_0 can be shown to have only a small effect on the final profile shape. In the early stages of growth, while the separation between bubbles remains relatively large, the bubbles grow without interaction with one another.

(ii) μ_0 and t_{dry}: μ_0 is the viscosity of the liquid at the start of the calculation. A "book" value for PU liquids is 100 poise or greater [7]. t_{dry} is a characteristic time for curing or drying. In the simulation the viscosity μ is taken to increase exponentially in time. The time constant for this process is t_{dry}. For times much larger than t_{dry}, the viscosity will be effectively infinite and the final profile shape will have been achieved.

(iii) σ_0 and K: σ_0 is the initial, assumed uniform, value of surface tension. The surface

tension is reduced locally by the presence of surfactant. For simplicity we assume that all of the surfactant molecules remain on the liquid-air interface and that their number is conserved. We also assume a linear relation of the form

$$\sigma = \sigma_0 - K\left(\Gamma - \Gamma_0\right) \tag{2.2}$$

where Γ is the local concentration of surfactant and is a calculated function of time and space. K and Γ_0 are constants. Since the actual functional relation between σ and Γ is smooth, such a point-slope linear relation is valid provided σ does not deviate too much from σ_0. Without loss of generality, the initial uniform concentration Γ_0 can be taken equal to one. Then the surfactant "strength," that is the reduction in surface tension per unit of surfactant concentration, is given by the value of K. K is measured in the same units as surface tension.

(iv) L_0 is the initial length of the computational cell. The computational cell is a portion of the unit cell. The latter is the basic building block of the two-dimensional expanding foam. The length L_0, and the other computational and unit-cell dimensions, are defined in Figs. 1 and 2. L_0 is, in fact, proportional to the starting bubble size, as shown in Fig. 2.

(v) U_0 and n: U_0 is the average value of drawing speed. The left end of the computational cell is considered to be fixed in space. As the foam expands, the right end of the cell, which is a symmetry line (see Fig. 1), moves to the right at speed U_e whose average value during the expansion phase is U_0. As the cell expands, the gas fraction F increases because the total area of the unit cell increases while the liquid area remains constant. n is an exponent that determines the shape of the speed versus time function.

(vi) t_{proc} is the *process time*, the time required from the start of the motion for expanding foam to completely fill the available space in a closed container, for example. In general, t_{proc} is smaller or much smaller than t_{dry}.

(vii) D_0 is the initial value of the diffusion constant for surfactant. The diffusive mechanism is assumed to be similar to Brownian motion. For this reason, the value of this constant will decrease as the bulk viscosity μ increases. Surfactant molecules are in contact with the underlying bulk liquid and an increase in bulk liquid viscosity should impede surfactant mobility as well. The inverse dependence of diffusivity on viscosity is given by Einstein's Law for Brownian processes [8].

Dimensional analysis allows the number of parameters to be reduced by three. In dimensionless form, the law (2.1) is

$$\frac{\bar{h}}{L_0} = f_1\left(\frac{\mu_0 U_0}{\sigma_0}, \frac{K}{\sigma_0}, F_0, \frac{t_{proc}}{T^*}, \frac{t_{dry}}{t_{proc}}, \frac{D_0 T^*}{L_0^2}, n\right) \tag{2.3}$$

where f_1 now denotes some other function. The characteristic time in (2.3) is

$$T^* = \frac{3\mu_0 L_0}{\sigma_0} \ . \tag{2.4}$$

The combination $Ca \equiv \mu_0 U_0/\sigma_0$ is a capillary number based on average drawing speed U_0. In the program the speed U_0 is not used directly. Instead it is replaced by the maximum window length L_{max} according to

$$U_0 = \frac{L_{max} - L_0}{t_{proc}} \tag{2.5}.$$

Then the capillary number is

$$Ca = \frac{T^*}{3t_{proc}} \left(\tilde{L}_{max} - 1 \right) \tag{2.6}$$

where $\tilde{L}_{max} = L_{max}/L_0$. $\tilde{L}_{max}$ will be related to the final gas fraction.

The dimensionless parameter K/σ_0 controls the strength of the surfactant effect. It has a strong influence on the final window thickness and shape. The present assumption, that the surfactant is insoluble in the bulk liquid, makes the surfactant very effective in controlling the stretching behavior of the liquid-gas interface. It will be seen that relatively small values of K/σ_0 will have a large effect on the dynamics of the film. This effectiveness would be reduced were surfactant solubility included in the model. The two time ratios in (2.3) can also be expected to have some effect on the final shape of the solidified film. Finally, $D_0 T^*/L_0^2 \equiv \tilde{D}$ is a dimensionless measure of diffusion of surfactant on the interface. Relatively large values of $\tilde{D}$ will decrease the effect of the surfactant and are expected to lead to thinner final films.

Similar to the situation for soap films [5], additional effects are expected here when portions of the films or windows become very thin. These effects are incorporated in a contribution to the total pressure in the liquid. This contribution is called *disjoining pressure* and represents a combination of Van der Waal's and other molecular forces and would also be influenced by the presence of surfactants [9]. The disjoining pressure function was introduced in the 1930's by the chemical physicists Frumkin and Deryaguin in order to better understand the origin of the static contact angle that appears where a sessile liquid droplet meets a solid substrate [10]. Note that, because of the way disjoining pressure is defined, a positive disjoining pressure is a negative contribution to the pressure applied to the liquid. The characteristic thickness scale for disjoining pressure Π is h_* and we use the five-parameter model

$$\Pi(h; h_*) = B_1 \left[\left(\frac{h_*}{h} \right)^{N-1} - \left(\frac{h_*}{h} \right)^{M-1} \right] \left(\frac{h_*}{h} - C \right) \ . \tag{2.7}$$

The constants have the following ranges: $B_1 \geq 0, \ N > M > 1, \ h_* > 0, \ 0 \leq C < 1.$

A repulsive pressure ($\Pi > 0$) is developed for $h < h_*$. A representative value for h_* is 10 *nanometers*. This repulsive pressure will tend to prevent window breakage. The magnitude of the disjoining effect is controlled by the prefactor B_1 which has the dimensions of pressure. Setting this parameter equal to zero will remove the disjoining effect entirely. In that case, corresponding to little or no surfactant effect, windows will break in the computer simulation. The two-term version of the disjoining model (*i. e.* C = 0) has been used in a variety of thin-film modeling studies [11, 12, 13, 5]. The disjoining pressure is attractive, or destabilizing, for $h_* < h < h_*/C$ and becomes repulsive (stabilizing) for $h > h_*/C$. $h \approx h_*$ is a stable energy minimum for this function, corresponding, for soap films, to the so-called *black film* thickness. The parameter C is introduced here for the first time. The two cases, C = 0 and $C > 0$, correspond to the two basic types of Π functions shown schematically in Teletzke *et al* [14]. Inclusion of C adds further generality to the model.

3. Initial Shape, Reference Parabola and Expanding Foam "Density"

The model assumes a two-dimensional geometry, corresponding to a plane section passed through a three-dimensional foam including thin films and Plateau borders. With the symmetry shown in Fig. 1, only a unit cell problem needs to be solved. For circular bubbles in hexagonal packing, the maximum area fraction corresponding to bubbles just touching is $F^* \approx 0.907$. We assume an initial area fraction $F_0 < F^*$. The corresponding radii are R^* and R_0. The initial unit cell is shown in Fig. 2.

While we use a circular bubble to specify the starting gas fraction F_0, the calculation employs the small-slope approximation and actually uses a parabola passing throught the point (L_0, b_0) that meets the 30^o symmetry line (at x = 0) in a right angle. The distance h_0 is changed somewhat by this replacement. Specifically, we use the parabola

$$\tilde{h} = \tilde{b} + \frac{1}{2\sqrt{3}} \ (\tilde{x} - 1)^2 \tag{3.1}$$

rather than the circular arc

$$\tilde{h} = 2 + \tilde{b} + \sqrt{4 - (\tilde{x} - 1)^2} \tag{3.2}$$

where

$$(x, h, b_0) = L_0 \ (\tilde{x}, \tilde{h}, \tilde{b}) \ .$$

The initial thickness used by the algorithm b_0 is related to the input volume or area fraction F_0

by

$$b_0 = R_0 \left(\sqrt{\frac{F^*}{F_0}} - 1 \right) \tag{3.3}$$

There is a small difference made by using the parabolic approximation rather than the circular arc. The maximum gas fraction for circles that just touch is $F^* \approx 0.907$. This number is reduced by about one per cent to 44/49 $\approx$ 0.898 when the parabolic arc is used in the definition. This difference is much less than the difference between two- and three-dimensional geometries where the maximum-packing *volume* fraction ≈ 0.75.

The calculation extends the liquid domain to the right at a prescribed rate while the liquid area, composed of the calculation domain $0 \leq x \leq L(t)$ and the smaller (shaded) 30-60-90 triangle in Fig. 2, is held constant. The gas fraction in the larger triangle increases as L increases. There is also a well-defined parabolic arc that meets the x-axis and encloses the same liquid area. The equation of this reference curve is

$$\tilde{h}_{ref} = \frac{1}{2\sqrt{3}\tilde{L}} \left(\tilde{x} - \tilde{L}_{ref} \right)^2 \tag{3.4}$$

where

$$\tilde{L}_{ref} = \sqrt{1 + \frac{28}{5}\sqrt{3}\ \tilde{b} + \frac{12}{5}\ \tilde{b}^2}\ . \tag{3.5}$$

For an expansion that happens slowly, without surfactant effect, and under certain other circumstances, the reference arc will closely approximate the final interface shape. Since the "film" thickness is identically zero, the reference arc would represent a window that will break.

One of the calculated quantities that is monitored as the simulation proceeds is the ratio d_f defined as

$$d_f = A_{liquid}/A_{cell} \tag{3.6}$$

where

$$A_{cell} = \frac{\sqrt{3}}{2} \left(L(t) + \frac{h_0(t)}{\sqrt{3}} \right)^2 \tag{3.7}$$

is the area of the unit cell and $h_0(t)$ is the thickness at $x = 0$ as shown in Fig. 2. A_{liquid} is a constant, independent of time, and is the area under the initial curve (3.2) plus the area of the smaller initial 30-60-90 triangle. d_f may be referred to simply as the foam *density*. This interpretation would give the correct numerical value of the density if the liquid has a specific gravity of one and the gas density is considered to be negligible. If this were the case, the dimensionless value d_f would be the foam density in tonnes/m^3.

4. Drawing Speed

The speed at which the right end of the computational window, as shown in Fig. 1, is moving to the right is an input function. This is the rate of stretching of the liquid portion of the unit cell. We use the function

$$L(t) = L_0 \left(1 + k \, \frac{t}{t_{proc}}\right)^n \qquad (0 \le t \le t_{proc}) \tag{4.1}$$

where t_{proc} is the process time, the time taken for the foam to fill the available space; *i. e.* for $t > t_{proc}$ the right end is stationary. Since $L = L_{max}$ at $t = t_{proc}$, the constant is

$$k = \left(\frac{L_{max}}{L_0}\right)^{\frac{1}{n}} - 1 \; . \tag{4.2}$$

The rate of expansion $U_e(t)$ is the actual variable used as the right-end boundary condition for the surface speed $U(x,t)$. It is

$$U_e(t) = \frac{dL}{dt} = nk \, \frac{L_0}{t_{proc}} \, \left(1 + k \, \frac{t}{t_{proc}}\right)^{n-1} \; . \tag{4.3}$$

It is assumed that experiments are performed and the rate of volumetric expansion dV/dt in a laboratory column, for example, is recorded. If the rate of expansion were observed to be constant, for example, and the number of cells does not change, then, since $V \sim L^3$, the exponent n would be 1/3. Perhaps more consistent with two-dimensional modeling, the areal expansion rate could be taken to be constant, in which case $n = 1/2$. In either of these cases, the speed would decrease with time. In a completely predictive model, the function $U_e(t)$ would be a calculated rather than an input function. It depends on the rate of gas generation due to reaction and, to a lesser extent, on the foam temperature history using the gas law.

5. Viscosification

Aqueous foams will continue to evolve in time indefinitely, albeit at a slow rate. Industrial foams, on the other hand, are made to solidify rather quickly. This solidification is accomplished, within the model, by a large increase in viscosity. Thus the portion of the model discussed in this section is only required for foams that solidify.

At early times the liquid viscosity is relatively small. Through one or several processes, the matrix material becomes a solid. Information on the chemistry of this *set-up* could be included in a more comprehensive process model. It could involve polymerization, loss of solvent ("drying"), thermal curing or other effects. The common feature is that the viscosity will increase in time, ultimately by many orders of magnitude. A solid can be thought of as a liquid of infinite viscosity.

The simplest model is one in which the viscosity μ is a function only of time. We choose the one-parameter model

$$\mu(t) = \mu_0 \exp\left(\frac{t}{t_{dry}}\right) \tag{5.1}$$

where t_{dry} is called a "drying time" and is an input parameter. We prescribe the ratio t_{dry}/t_{proc} as the input quantity. With the assumed exponential dependence, when t is a significant multiple of t_{dry}, the viscosity will be high enough that the liquid will cease to move and the final film shape is given by the simulation. We expect that t_{dry} will be several times larger than t_{proc}. To the extend that this is true, once the extension has stopped, the effect of viscosification can be absorbed by changing the time scale. This means that the profile for a liquid of constant viscosity at any time could be the final profile for an appropriately selected value of t_{dry}. During the pulling phase, on the other hand, the profile shape is influenced both by viscous draining and the rate of pulling; thus there is a nonlinear interaction between the two effects that is determined by the numerical simulation. In general we expect that rapid drying will lead to thicker films because capillary-driven backflow into the Plateau borders is inhibited.

With the model in (5.1) the liquid is still Newtonian. Zhang, Davis & Macosko [6] suggest that PU material is shear-thinning because of urea precipitation. Shear thinning is perhaps not the right word since it presupposes a shear-dominated flow. Extensional thinning is more appropriate for mobile interfaces (small surfactant effect) since the flow is largely extensional for that case. In either event, the viscosity is a decreasing function of strain rate and will then also vary in space as well as time. This effect, usually referred to as *generalized Newtonian* [see Bird *et al* [15]], can be considered within the lubrication model. This generalization is considered in section 8 where a so-called Ellis model is added to the numerical model [16, 17].

Another alternative could be called a "paint drying model." In this case, the viscosity increases as a particular component of the mixture, *i. e.* a solvent, is lost from the liquid. Since the loss is through the interface, thinner portions can be expected to dry faster. Thus the viscosity in the thinnest portion of the film will increase most rapidly. This will also lead to thicker films, we believe. Since the viscosity is a function of the bulk concentration of a given element of liquid (*i. e.* how dry it is) and since these elements move, it would be necessary to include the bulk concentration as an additional unknown in the model. This has been modeled for the simpler problem of paint drying [18].

For a Newtonian or generalized Newtonian liquid, the viscosity depends at most on the state of dryness or cure and the instantaneous local rate of deformation. It is possible that the

viscosity could also depend on the previous history of the motion. Polymerization could add elasticity to the matrix material. A one-dimensional visco-elastic model of Maxwell-type is suitable to approximate a flow that is primarily extensional. It will require that the local state of strain be monitored along the film as the calculation proceeds. This information can be extracted from the numerical algorithm.

6. Mathematical Model; Differential equations and boundary conditions

Three coupled nonlinear partial differential equations determine the temporal and spatial variation of the profile $h(x,t)$, the surface speed $U(x,t)$ and the surfactant concentration $\Gamma(x,t)$. These equations are derived, starting from the Stokes equations for slow motion of viscous fluids, and the pressure and kinematic free-surface conditions, by Schwartz & Roy [5]. The major simplification employed there is the use of the small-slope *lubrication* approximation. Mathematical derivations of the basic approximation are given by Benney ([19]) and Atherton & Homsy ([20]). The boundary conditions used here, at the Plateau border and the moving end, are, however, quite different from the earlier work. It may also be noted that inertial, *i. e.* finite-Reynolds number, effects are quite negligible for the present problem.

6.1 The h-evolution equation

The evolution equation for the film shape is

$$h_t = -Q_x = -(Uh)_x - \frac{\sigma}{3\mu}\left[h^3\left(h_{xxx} + \frac{\Pi_x}{\sigma}\right)\right]_x . \tag{6.1}$$

where subscripts signify partial differentiation. The first equality is the condition of mass conservation for the assumed constant-density liquid. Q is the areal flux, defined as

$$Q(x,t) = \int_0^{h(x,t)} u(x,y,t)\, dy$$

where the coordinate y is measured from the film centerline and u is the velocity component in the x direction. The first term on the right of (6.1) contains the convective contribution Uh_x and the domain-stretching effect hU_x. The second term is the pressure gradient contribution to Q and consists of the capillary component, using the surface curvature gradient h_{xxx}, and the disjoining component using the function Π given in equation (2.7).

Equation (6.1) can be made dimensionless using L_0 as the characteristic length for both h and x and $T^* = (3\mu_0 L_0)/\sigma_0$ as the characteristic time from (2.4). The dimensionless variables are formed, of course, by dividing the original dimensional quantities by the appropriate

reference quantity. Several physical parameters in the original system are seen to be removed by this transformation. Using the new dimensionless variables, (6.1) be

$$h_t = -(Uh)_x - [h^3(h_{xxx} + \Pi_x)]_x \ . \tag{6.2}$$

The two left-end (Plateau border) boundary conditions are:
(i) The slope is given for all time at $x = 0$,

$$h_x(0,t) = -\tan(\pi/6) \ . \tag{6.3}$$

(ii) The smaller 30-60-90 triangle area A_Δ in Fig. 2 is related to the flux at $x = 0$ which is denoted by $Q(0)$. Thus

$$Q(0) = -\frac{dA_\Delta}{dt} \ \ ; \ \ A_\Delta(t) = \frac{h^2(0,t)}{2\sqrt{3}} \ . \tag{6.4}$$

The moving-end boundary conditions are the symmetry condition

$$h_x(L(t),t) = 0 \tag{6.5}$$

and the flux condition

$$Q(L(t),t) = h(L(t),t)\ U_e(t) \tag{6.6}$$

where U_e is given by (4.3) for $t < t_{proc}$ and U_e = 0 for $t \geq t_{proc}$. The initial shape $h(x,0)$ is given by equation (3.1).

6.2 The equation for the surface speed

Consider first the simplest case, a viscous liquid sheet being drawn out by a constant tension per unit width T. If no other forces are present, the normal stress τ_{11}, on a sheet whose thickness is almost uniform, satisfies the stress-strain rate relation

$$\tau_{11} = T/h = 4\mu U_x$$

where T is the (half) film tension [15]. The quantity 4μ is sometimes called the Trouton viscosity for this extensional process. h is the (half) film thickness. The stretching velocity is zero at the Plateau border and is a specified function of time $U_e(t)$ at the line of symmetry.

Thus, for force equilibrium $T =$ constant, and U satisfies

$$(hU_x)_x = 0 \tag{6.7}$$

and the boundary conditions

$$U(0,t) = 0, \qquad U(L,t) = U_e(t)\ . \tag{6.8a,b}$$

Since hU_x is constant along the sheet or film, it follows immediately that the rate of elongation varies inversely with the thickness h. Thus thin regions of the film will thin most rapidly and it will not be possible to extend the film, or expand a foam, to any appreciable degree because film thicknesses will become catastrophically small. In fact, it is the presence of surfactant, and the resulting surface tension gradient forces, that makes foam expansion possible.

Following Schwartz & Roy [5], we use instead a more complete model that includes surface traction due to nonuniform surfactant, finite capillary pressure, and disjoining pressure. The surface traction is

$$\tau = \frac{\partial \sigma}{\partial x}$$

within the small-slope approximation [8]. Using (2.2), the traction is $\tau = -K\ \Gamma_x$ and we perform a force balance on an element of film. Instead of (6.7), the stretch speed now satisfies

$$4\mu(hU_x)_x + h(\sigma h_{xxx} + \Pi_x) - K\Gamma_x = 0\ . \tag{6.9}$$

In dimensionless variables, using L_0 as the reference length for x and h and $T^* = (3\mu L_0)/\sigma_0$ as the characteristic time, as before, (6.9) becomes

$$(hU_x)_x = -\frac{3}{4}\ (h\ h_{xxx} + h\Pi_x) + (K/\sigma_0)\Gamma_x\ . \tag{6.10}$$

We have made the approximation $\sigma \approx \sigma_0$. This is equivalent to stating that the fractional change in surface tension, due to the presence of surfactant, is small. For systems of small physical dimensions, such as those considered here, it is possible to have large values of $\partial\sigma/\partial x$ even though the change in σ is small. Note that, since (6.10) is an *elliptic* rather than a *parabolic* differential equation, no initial condition can, or should, be specified for $U(x,t)$. This follows from the consistent neglect of inertial effects in the present theory.

The dynamical behavior of the stretching liquid films becomes simple in an important limiting case. The physical reason for this simplification is clear. Assume a uniform initial distribution of surfactant. If the surfactant effect is strong, the stretched surface must also have an almost uniform distribution, because any nonuniformity will give rise to a strong traction tending to restore uniformity. This implies that, within the small-slope approximation, the

rate of dilation dU/dx is constant or $U(x,t) = kx$, where k is some constant. This uniform dilation, with a fixed point at $x = 0$, is referred to mathematically as an *affine transformation*. Results of a separate calculation, using the affine stretching assumption, will be given below and compared with results of the more complete theory. This simple argument neglects the weakening effect of surface diffusion of surfactant. It will be demonstrated using the results of the computer simulation, shown below in section 7, that this is the correct limiting behavior when the surfactant effect is strong.

6.3 The surfactant concentration convection-diffusion equation

As in Schwartz & Roy [5], the surfactant concentration satisfies

$$\Gamma_t = -(U\Gamma)_x + D(t)\,\Gamma_{xx}\ . \tag{6.11}$$

Because this equation is linear in Γ, the units of Γ are irrelevant since the boundary conditions are also homogeneous. These boundary conditions are

$$\Gamma_x(0,t) = \Gamma_x(L(t),t) = 0\ . \tag{6.12}$$

The first of these follows from the observation that the left end of the free surface lies on an inclined symmetry axis, as in Fig. 1. On that inclined axis, $d\Gamma/ds = 0$ where s is arc length along the interface. Since the slope there is finite, $\Gamma_x = 0$ there as well. The right-end boundary condition is also $\Gamma_x = 0$, irrespective of whether the boundary is moving or stationary, since this boundary is also a line of symmetry. The initial condition is that the surfactant is uniformly distributed, *i. e.* $\Gamma(x,0) = \Gamma_0 = const.$ Without loss of generality, Γ_0 can be taken equal to one.

It may be verified, using the differential equation and boundary conditions, that the total quantity of surfactant is conserved. Consider

$$\frac{d}{dt}\int_0^{L(t)} \Gamma\ dx = \int_0^{L}\ \Gamma_t\ dx + \Gamma(L)\ \frac{dL}{dt} \tag{6.13}$$

using Liebnitz' rule for differentiating under the integral sign. Substituting the differential equation in the integral on the right and noting that $dL/dt = U(L,t) = U_e(t)$, we find

$$\frac{d}{dt}\int_0^{L(t)} \Gamma\ dx = -U(L)\ \Gamma(L) + U(0)\ \Gamma(0) + D\left[\Gamma_x(L) - \Gamma_x(0)\right] + \Gamma(L)\ U(L)\ . \tag{6.14}$$

But $U(0)$ =0 from (6.8) and the first and last terms on the right of (6.14) are seen to cancel.

Thus, with the boundary condtions (6.12), we have

$$\int_0^{L(t)} \Gamma \, dx = \Gamma_0 \, L_0 = const \; . \tag{6.15}$$

The value of the constant is one in dimensionless variables.

7. Some sample results

Figures 3 through 6 show the film profile h, the surface speed U and the surfactant distribution Γ at a particular time. The surfactant strength is varied, yielding a family of curves for each of these quantities. We arbitrarily select the time instant when the profile length has doubled during the stretching phase of motion. In the finite-difference calculations, the point spacing Δx is held constant as the liquid film is stretched. Thus additional points are added continuously as the simulation proceeds. The surfactant level is given, in effect, by specifying K/σ_0 which will be symbolized by G in the figures. Apart from this quantity, the non-dimensional input parameters are listed in the following table:

Table I: Parameter values used to create simulation results

`0.85`	F	Initial gas fraction
`3.0`	L_{max}/L_0	Maximum cell length
`100.`	t_{proc}/T^*	Dimensionless process time
`0.01`	$B_1/(\sigma_0/L_0)$	Disjoining prefactor
`0.0001`	h_*/L_0	Disjoining thickness
`0.1`	DT^*/L_0^2	Surfactant diffusion constant
`4.`	N	Stable disjoining exponent
`3.`	M	Unstable disjoining exponent
`0.5`	C	Disjoining stabilization constant
`1.`	n	Exponent in stretching law $L/L_0 = (1 + Ct)^n$
`10.`	t_{dry}/t_{proc}	"Drying" time ratio

The system of three coupled partial differential equations in section 6 is solved numerically by the method of finite differences. The computer code is written in the Fortran language. The computation is started using 100 equally-spaced points to represent the surface ordinates, the surfactant distribution and the surface speed. Points are added, as the stretching proceeds, so that 300 points are ultimately used for each variable. Time marching is done implicitly in the sense that a system of algebraic equations is solved for the incremental changes at each time step. A complete evolution history, for a given set of input parameters, can be obtained in less

than one minute using a 1.2 GHz desktop computer and the Linux public-domain operating system.

It is instructive to suggest some representative physical values, similar to those given in [7]. Assume L_0 = 0.01 cm, σ_0 = 30 dynes/cm and μ_0 = 100 poise = 100 gm/(cm sec). Then the characteristic time is T^* = 0.1 sec using equation (2.4). The tabular value for the process time is then 10 sec which seems to be a reasonable value. The characteristic time for drying or solidification is then 100 sec. The disjoining thickness h_* is taken to be 10^{-6} cm, equivalent to a 20 nm total thickness for the "two-sided" film. This is a satisfactory value, at least in an order-of-magnitude sense. This value is large by a factor of between two and four for black soap films, however [21]. For the initial gas fraction and maximum cell length given in the table, the final gas fraction is 0.978; thus the foam "density" is 0.022. The large gas fraction means that this is a "high-quality" foam.

Figure 3 is a snapshot of the film profile, h/L_0 versus x/L_0, at a time during the expansion when the film length has doubled, *i. e.* when $L = 2L_0$. Note that the vertical scale is exaggerated by about a factor of three. Four separate curves are shown, corresponding to different levels of the surfactant strength parameter $G = K/\sigma_0$ that appears in equation (6.10). G = 0 is the case of zero surfactant strength; consequently, in this case, there is no surface shear stress resulting from spatial nonuniformity in the surfactant distribution $\Gamma(x,t)$. An additional curve, labelled "affine" is also shown. It is calculated based on the assumption that the surface stretches uniformly, as discussed in section 6.2. This assumption holds when the surfactant effect is relatively strong. In this case the motion may be decomposed into a linear combination of affine stretching and a motion that satisfies a no-slip condition on the liquid-gas interface. The film stretching can then be calculated using only the single evolution equation

$$h_t = -(Uh)_x - \frac{\sigma}{3\mu}\left(h^3 h_{xxx}\right)_x \tag{7.1}$$

where U is given by

$$U(x,t) = U_{max}(t)\ \frac{x}{L(t)}\quad . \tag{7.2}$$

The recognition that flow with a surfactant-laden interface must satisfy a no-slip condition on that interface, and is therefore analogous to film flow on a solid substrate, may be found in Mysels *et al.* [2].

The information in Fig. 3 is replotted in Fig. 4 using a logarithmic scale to more clearly illustrate the important effect of the surfactant. The film thicknesses for no surfactant (G = 0) and the case of G = 0.001 can be seen to differ from one another by at least a factor of 100. In fact, for G =0, the computation would have failed, with the thickness h going to zero at some point, has the relatively weak disjoining pressure term not been present in the thickness evolution equation (6.1). Note also the close agreement between the result of the affine calculation and the profile for G = 0.001. It is perhaps surprising that this rather modest

surfactant effect is sufficient to effectively immobilize the interface.

Figure 5 shows the interfacial speed variation $U(x/L_0)$ at the same "snapshot" time for which the h profiles are shown. Note that the calculated speed variation for the largest G value is virtually a straight line, confirming the validity of the affine stretching hypothesis. Note that U can become negative, implying backflow into the Plateau border, when G is small. Over a certain portion of the film length, therefore, liquid is being removed in both the forward and backward directions. This is the origin of the thickness minimum or "dimple" that can often persist until the film has dried. Dimples in the final dry profiles, for small G values can be seen in Fig. 7.

Figure 6 shows the distribution of surfactant $\Gamma(x/L_0)$ at the same snapshot time for the four different values of G. These distributions are calculated using the convection-diffusion equation (6.11). In the numerical model the diffusion constant D is reduced as the viscosity increases with time, consistent with Einstein's law for diffusion [8]. This reduction does not appear to be an important effect, however. Since surfactant is assumed to be conserved, the area under each curve in Fig. 6 should be the same. Some error in the total quantity of surfactant is apparent in the figure. This error is about 2 per cent and arises because the four separate runs were terminated manually and the stopping time was not exactly the same in each case. Note that, for the largest G value, the surfactant is distributed almost uniformly, as expected.

The final shapes, after the film has been pulled to three times its original length and allowed to dry, are shown in Fig. 7. The three previously-used values of surfactant strength G all display a thickness minimum. Results for two larger G values are also shown, demonstrating that the "dimple" can be avoided if desired. Moreover, it is clear that increasing G from 0.01 to 0.1 has almost a negligible effect on the final film profile. Thus it follows that there is a maximum window thickness that can be achieved using surfactant. Once this level is reached, there is no useful purpose served by further addition of surfactant.

The foam expansion process is illustrated more dramatically in Fig. 8. Here the initial shapes of four circular bubbles, at a gas fraction of 0.85, are compared with the final pattern. The value of G is 0.0001. The bubble shapes were recovered from the unit-cell results by use of the appropriate reflections, translations, and repetitions. The fully-expanded bubble profile is taken from the one shown in Fig. 7 for the same value of G.

8. Incorporation of certain Non-Newtonian flow effects

Equations (6.1) and (6.9) are based on an assumed Newtonian rheology for the liquid. The viscosity changes only globally with time to simulate solidification or drying. However, it is expected that in a PU foam, for example, the liquid phase actually exhibits more complex rheological behavior. Such behavior may affect the cell opening characteristics of the foam via increased film thinning and consequent window breakage. During the expansion of a PU foam,

polymeric urea is known to precipitate to form a separate phase within the polymer network. There is evidence that, at some point during the reaction, the resulting foam matrix consists of a suspension of urea particles with strong shear thinning and extensional thinning behavior. The locations of stress concentration which occur at the dimples of the film during expansion are accompanied by a local lowering of the viscosity, and hence by a further weakening of the film. Therefore, one may conclude that urea precipation plays a contributory role in cell opening. See Zhang, Davis & Macosko [6] for further discussion and experimental evidence.

In order to incorporate this effect into the model, we choose the generalized Newtonian Ellis model discussed by Bird *et al.* [15]. The model can be expressed using the following relationship between the (shear) viscosity μ and the shear-stress τ:

$$\mu(x,t) = \frac{2\mu_1}{1+|\tau/\tau_0|^{\alpha-1}} \tag{8.1}$$

where τ_0, and α are constants. The vertical bars signify absolute value. μ_1 is spatially constant at any given time and is, in fact, given by the previous solidification law (5.1). Note that the Newtonian model is recovered by setting $\alpha = 1$. Shear-thinning behavior is obtained when $\alpha > 1$. Unlike the previous simpler model given above, the viscosity now varies in space as well as time.

It can be shown that evolution equation (6.1) for the film shape becomes

$$h_t = -(Uh)_x - \frac{dQ_\sigma}{dx}, \frac{\partial Q_\sigma}{\partial x} = \frac{h^3}{3\mu_1}\, S(x)\, (\sigma h_{xxx} + \Pi_x) \tag{8.2}$$

where the prefactor $S(x)$ is given by

$$2S(x) = 1 + \frac{3}{\alpha+2}\left(\frac{h}{\tau_0}|\sigma h_{xxx} + \Pi_x|\right)^{\alpha-1} \tag{8.3}$$

Again equation (6.1) is recovered by setting $\alpha = 1$.

In order to extend equation (6.9) to the generalized Newtonian case, we postulate that the extensional viscosity is given by 4μ, the so-called "Trouton viscosity" for a Newtonian liquid. Equation (6.9) governing the surface speed now becomes

$$4(\mu\, hU_x)_x + h(\sigma h_{xxx} + \Pi_x) - K\Gamma_x = 0, \qquad \frac{2\mu_1}{\mu} = 1 + \frac{3}{\alpha+2}\left(\frac{h}{\tau_0}|\sigma h_{xxx} + \Pi_x|\right)^{\alpha-1} \tag{8.4}$$

where now the extensional viscosity is also a function of both space and time. Note that the Newtonian case can also be obtained from the Ellis model in the limit $\tau_0 \to \infty$. Then a Newtonian rheology is approached with viscosity equal to $2\mu_1$.

Figure 8 shows the effect of increasing the parameter α, and hence making the liquid increasingly non-Newtonian, while keeping all other parameters constant. Parameter values are somewhat different from those used for the Newtonian case discussed above. These differences produce only minor quantitative changes, when compared with more dramatic effects due to localized viscosity reductions. In particular, the simulation of Fig. 8 used $L_{max}/L_0 = 4$, t_{proc}/T^* = 800, t_{dry}/t_{proc} = 2.5 and G = 0.0017. The figure shows final dry film profiles. As α is increased, the flat part of the film becomes markedly thinner and the dimples become deeper. Thus when this non-Newtonian effect is considered, windows will have a greater tendency to break. It may be that an open-cell or partially open-cell foam will result when a closed cell foam might otherwise have been anticipated.

9. Concluding remarks

We have developed a theoretical and numerical model for the growth, shape evolution and ultimate solidification of a foam. Although the model embodies many simplifying assumptions, we believe that it is currently capable of making quantitative predictions concerning the influence of changes in gas injection rates, surfactant strength, fluid rheology, and other process variables. At a minimum, the current model should serve as an appropriate stimulus for further work.

It is necessary to point out some limitations of the present model. It deals principally with the description of *fluid dynamic behavior* as driven by a known rate of gas production. In a more completely predictive model of an exothermally expanding foam, simplified models of the chemical and thermal processes, that can be used to predict the gas production rate, could be incorporated. The present assumption that the liquid volume remains constant could then also be removed and replaced by a calculated mass transfer history.

The presently-used assumption, that the surfactant is insoluble in the bulk liquid, is felt to be an oversimplification that is likely to be more appropriate for soap surfactants (fatty acids) that it is for PU foam constituents. A more complete model could incorporate transfer of surfactant between the interface and the bulk liquid. A simple way of capturing a portion of the effect of transfer of surfactant between the interface and the bulk liquid film is to use a simple "reservoir" model. A single term can be added to equation (6.11) so that it becomes

$$\Gamma_t = -(U\Gamma)_x + D\,\Gamma_{xx} - D_b(\Gamma - \Gamma_b) \tag{9.1}$$

where D_b is a type of "bulk diffusion constant" and Γ_b is a reference or reservoir value. If the interfacial concentration Γ becomes less than Γ_b, the bulk supplies surfactant to the interface at a rate proportional to D_b; conversely surfactant is lost to the bulk whenever $\Gamma > \Gamma_b$. This change is straightforward to implement. This more complete model has been used previously [22]. It may be criticized, however, because for very thin films the reservoir supply of surfac-

tant may be insufficient to maintain a constant value of Γ_b. A more complete model would consider the bulk concentration Γ_b as an unknown, to be found through the use of another convection-diffusion equation [23].

The significant geometric simplification incorporated in the present model needs to be appreciated. We have replaced a complex three-dimensional matrix structure with a two-dimensional idealization and have also postulated a high degree of symmetry. It is possible to extend the model to incorporate certain three-dimensional features. Gravity drainage, for example, would need to be included, along a network of struts, for an aqueous or slow-drying foam. Then the small-scale problem treated here could still be appropriate, provided that the liquid mass conservation conditions are suitably modified; the total liquid area in the two-dimensional problem would no longer be constant. It is also possible in principle to replace the present Newtonian or generalized Newtonian liquid with a more general model that will allow the viscosity to vary in space in response to changes in both the rate of deformation and the local deformation history. This latter dependence is usually referred to as *viscoelasticity*. Viscosity can also be made to vary in space as a function of the evolving mixture composition. Note that the initial size of an expanding bubble is assumed to be a known quantity. We are not currently attempting to model the initial stages of nucleation and growth of bubbles, including any possible gaseous exchange mechanism such as *Ostwald ripening*, that can occur then.

One goal is the identification of unrealistic assumptions in the present model in order to suggest the most important model improvements. Model predictions can be compared with micrographs of actual expanded foams. Various diagnostic experiments that can be designed and performed to validate and improve the present model. We believe that the model is, or will shortly become, capable of yielding improved understanding that can lead to improved processing and new products. Benefits may include the possibility of very low density foams, as well as potential cost savings by careful control of expensive mixture constituents such as surfactants.

Acknowledgment

This work was supported by ICI and Huntsman-ICI Polyurethanes. The support, and permission to publish these results, is gratefully acknowledged.

References

[1] D. Weaire, S. Hutzler, G. Verbist, and E. Peters. A review of foam drainage. *Adv. Chem. Phys.*, 102:315–373, 1997.

[2] K. Mysels, K. Shinoda, and S. Frankel. *Soap Films, Studies of Their Thinning*. Pergamon, New York, 1959.

[3] L. W. Schwartz and H. M. Princen. A theory of extensional viscosity for flowing foam. *J. Coll. Interface Sci.*, 118:201–211, 1987.

[4] L. W. Schwartz, R. A. Cairncross, and D. E. Weidner. Anomalous behavior during leveling of thin coating layers with surfactant. *Phy. of Fluids*, 8(7):1693–1695, 1996.

[5] L. W. Schwartz and R. V. Roy. Modeling draining flow in mobile and immobile soap films. *J. Coll. Interface Sci.*, 218:309–323, 1999.

[6] X. D. Zhang, H. T. Davis, and C. W. Macosko. A new cell opening mechanism in flexible polyurethane foams. *J. Cellular Plastics*, 35:458–476, 1999.

[7] G. Woods. *The ICI Polyurethanes Book*. John Wiley, Chichester, 1990.

[8] L. D. Landau and E. M. Lifshitz. *Fluid Mechanics*. Pergamon Press, Oxford, 1959.

[9] J. N. Israelachvili. *Intermolecular and Surface Forces*. Academic Press, London, 1992.

[10] N. V. Churaev and V. D. Sobolev. Prediction of contact angles on the basis of the Frumkin-Derjaguin approach. *Adv. in Coll. and Interface Sci.*, 61:1–16, 1995.

[11] V. S. Mitlin and N. V. Petviashvili. Nonlinear dynamics of dewetting: Kinetically stable structures. *Phy. Let. A*, 192(5-6):323–326, 1994.

[12] L. W. Schwartz and R. R. Eley. Simulation of droplet motion on low-energy and heterogeneous surfaces. *J. Coll. Interface Sci.*, 202:173–188, 1998.

[13] A. Sharma. Equilibrium and dynamics of evaporating or condensing thin fluid domains: thin film stability and heterogeneous nucleation. *Langmuir*, 14:4915–4928, 1998.

[14] G. F. Teletzke, H. T. Davis, and L. E. Scriven. Wetting hydrodynamics. *Revue de Physique Appliquee*, 23(6):989–1007, 1988.

[15] R. B. Bird, R. C. Armstrong, and O. Hassager. *Dynamics of Polymeric Liquids*. Wiley, New York, 1977.

[16] D. E. Weidner. *Numerical simulation of coating flows*. PhD thesis, University of Delaware, 1993.

[17] D. E. Weidner and L. W. Schwartz. Contact-line motion of shear-thinning liquids. *Phy. of Fluids*, 6:3535–3538, 1994.

[18] M. H. Eres, D. E. Weidner, and L. W. Schwartz. Three-dimensional direct numerical simulation of surface-tension-gradient effects on the leveling of an evaporating multicomponent fluid. *Langmuir*, 15(5):1859–1871, 1999.

[19] D. J. Benney. Long waves on liquid films. *J. of Math. and Phy.*, 45:150–155, 1966.

[20] R. W. Atherton and G. M. Homsy. On the derivation of evolution equations for interfacial waves. *Chem. Eng. Comm.*, 2:57–77, 1976.

[21] I. B. Ivanov. *Thin liquid films; fundamentals and applications*. Marcel-Dekker, New York, 1988.

[22] P. L. Evans, L. W. Schwartz, and R. V. Roy. A mathematical model for crater defect formation in a drying paint layer. *J. Coll. Interface Sci.*, 227(5):191–205, 2000.

[23] V. G. Levich. *Physiochemical Hydrodynamics*. Prentice-Hall, Inc., Englewood Cliffs, 1962.

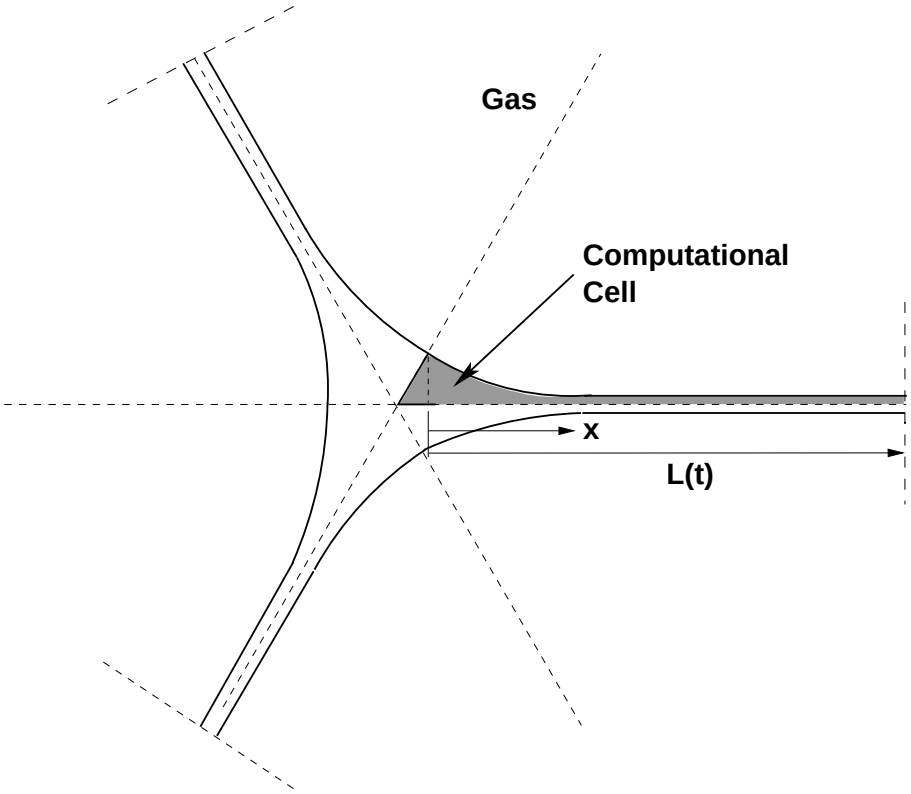

Figure 1: Definition sketch of stretched films and Plateau borders at time t. Initially the computational cell was smaller and the initial length was $L(0) = L_0$. At the initial time the gas bubble shapes were circular arcs. The six-fold symmetry is maintained during the stretching.

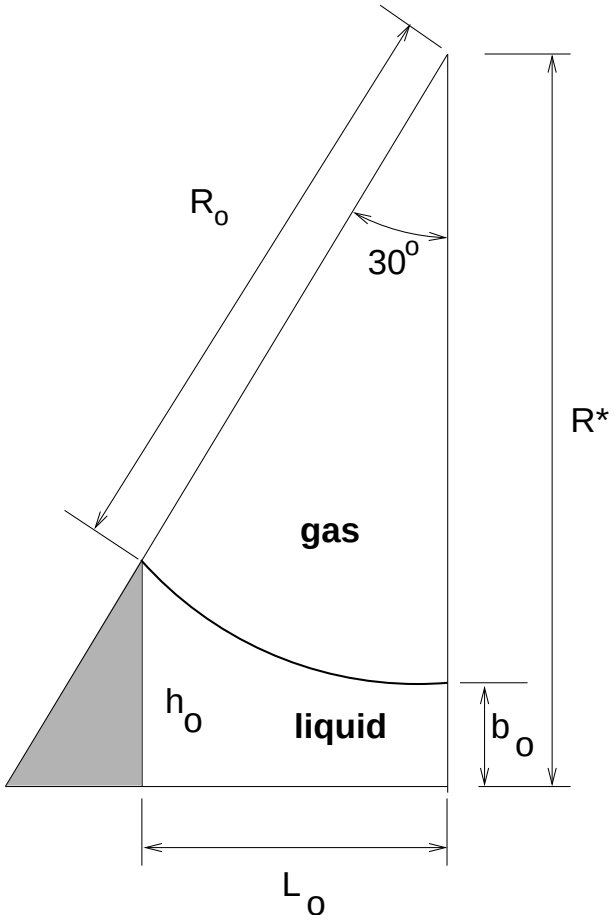

Figure 2: Initial (t = 0) configuration of the unit cell. R_0 is the starting radius of a two-dimensional bubble. $L_0 = R_0/2$ is used as the reference length in dimensionless calculations. R^* is the maximum circular radius of bubbles that just touch. The *stand-off* distance is $b_0 = R^* - R_0$.

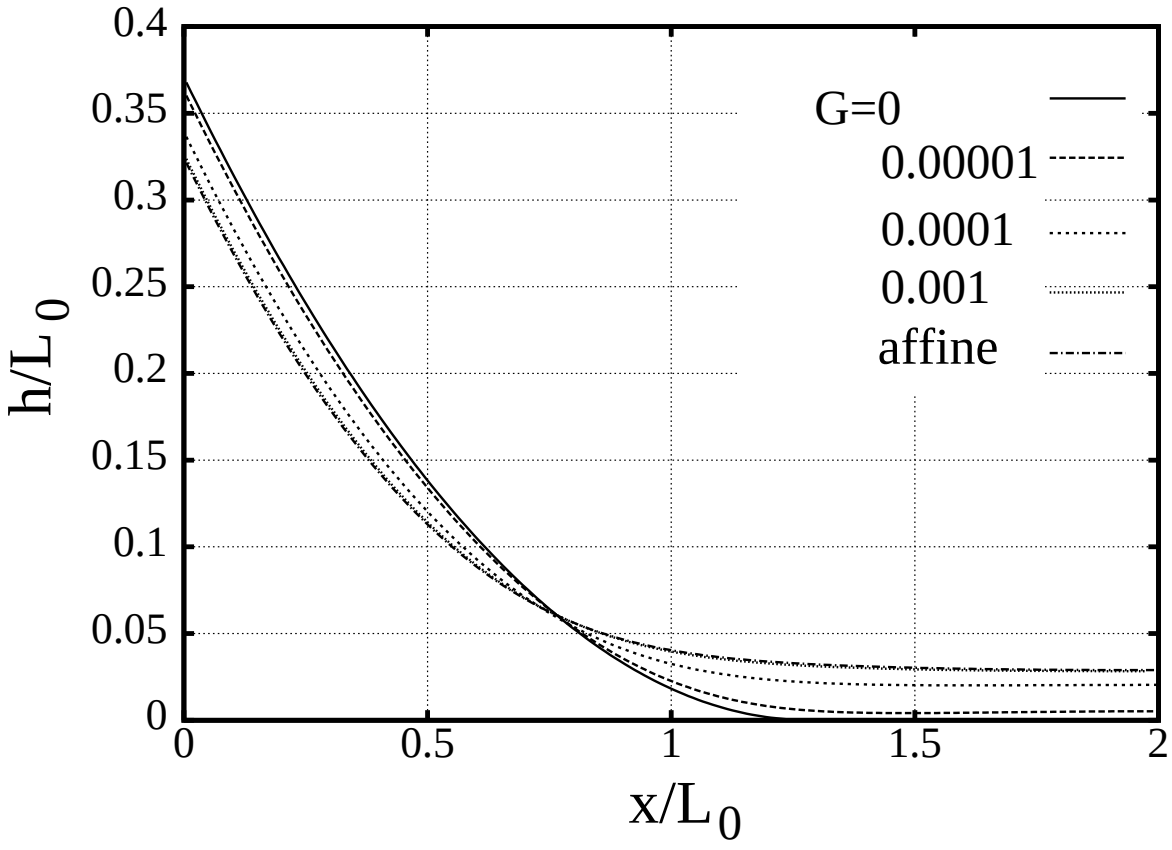

Figure 3: Dimensionless film thickness versus length from border. This is a snap-shot at the time instant when $L/L_0 = 2$. Four different surfactant levels are compared corresponding to different values of G. The profile for the highest surfactant level, $G = 0.001$, is close to the one labelled "affine." The affine profile is calculated using the assumption that the surface speed is given by $u/u_{max} = (x/L)$ where u_{max} is a constant and $L = L(t)$. According to the present model, the affine case is a "hardened" or no-slip interface and produces the thickest possible film. Reducing the strength of the surfactant effect results in thinner films.

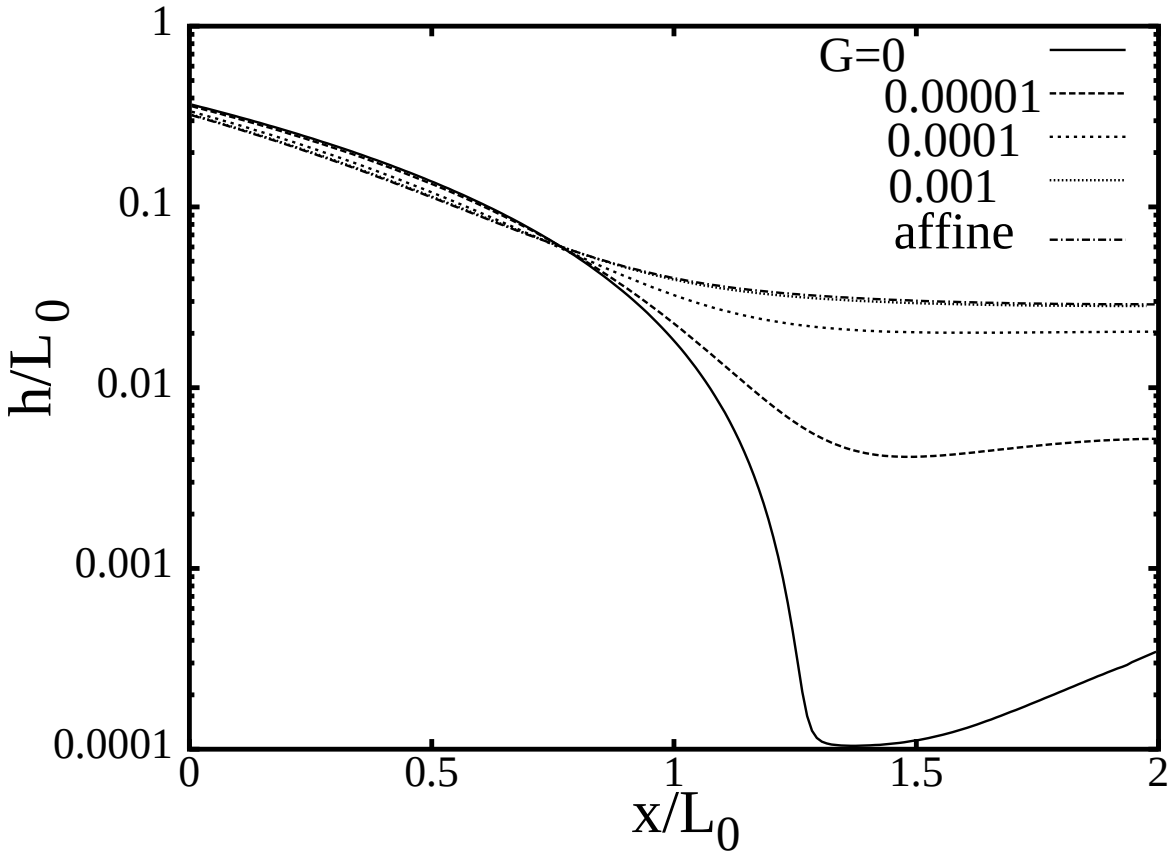

Figure 4: Film thickness h/L_0 versus position x/L_0 as in the previous figure. Here a log scale is used to more clearly illustrate the thickness variation of the film and how it depends on the surfactant level G. The thinnest film would eventually break were it not for the disjoining pressure that is included in the model.

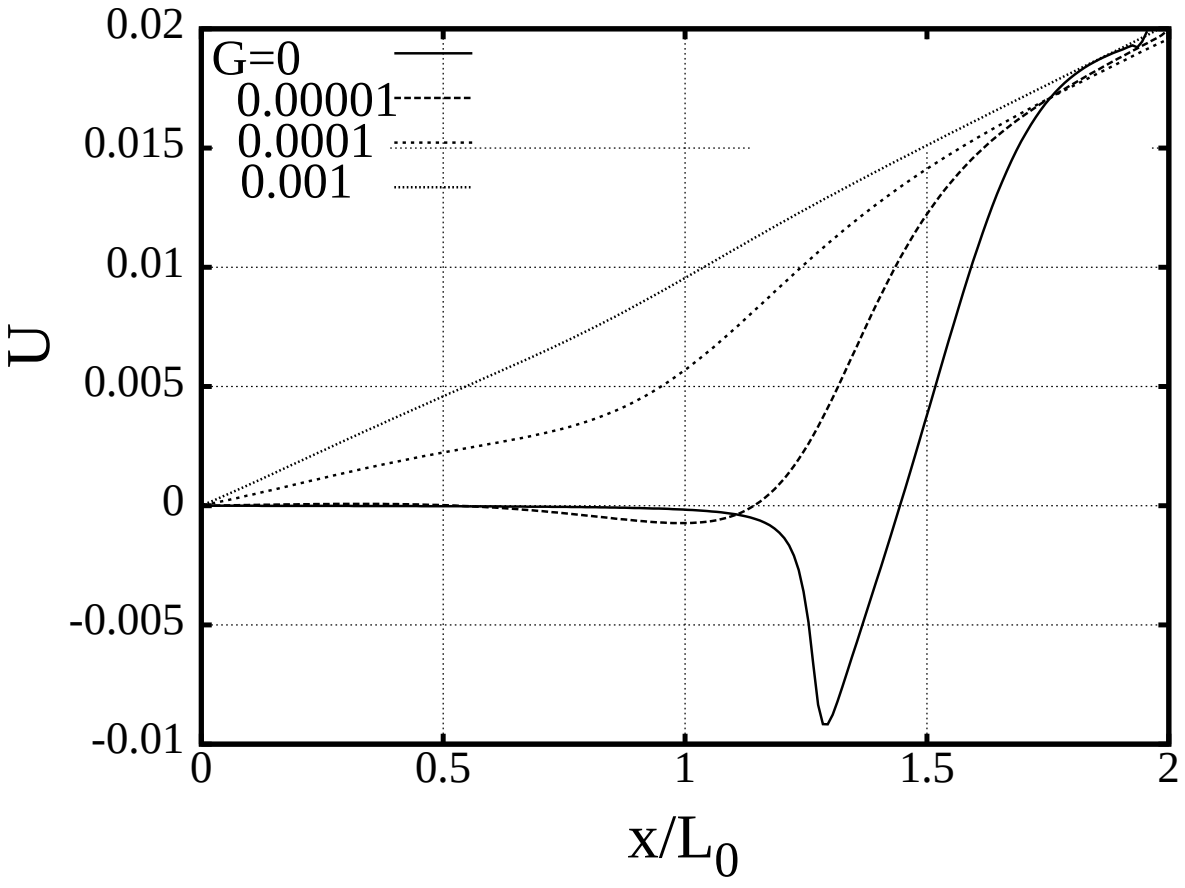

Figure 5: Dimensionless surface speed U versus x/L_0 for several surfactant levels G. $L/L_0 = 2$ at dimensionless time $t \approx 0.5$ corresponding to the h profiles shown in Figs. 3 and 4. For the the highest surfactant level shown, the profile is virtually linear, justifying the so-called affine assumption. For little or no surfactant, there is backflow towards the Plateau border. This backflow can even occur during the expansion phase, as demonstrated here, if the surfactant effect is quite weak. When backflow occurs during the expansion phase, the flow must change direction at a certain position. This may lead ultimately to formation of a thickness minimum or "dimple" in the final profile.

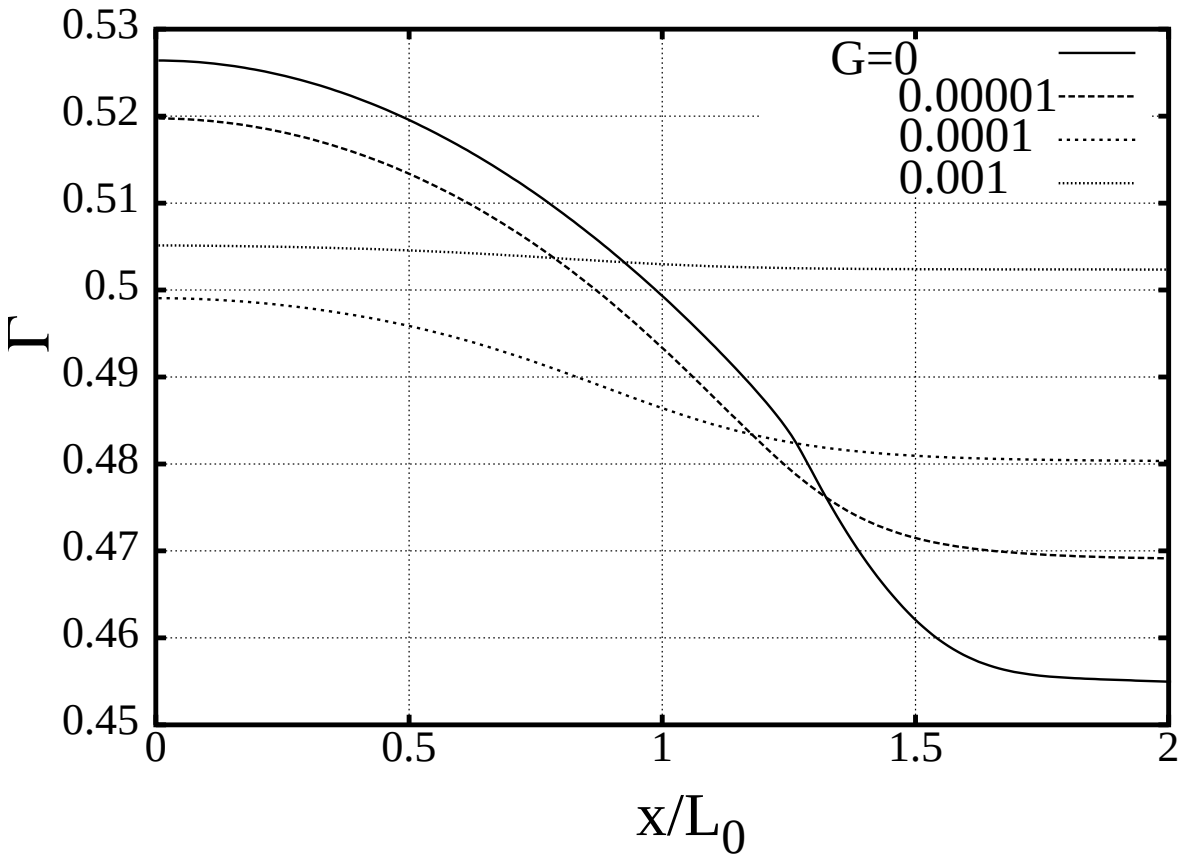

Figure 6: Surfactant distribution Γ versus x/L_0 for different levels of surfactant effect; $L/L_0 = 2$. The total quantity of surfactant is normalized to one. Slight differences in the average value shown here are because the runs were stopped at slightly different times. For the strongest surfactant effect shown, the surfactant distribution can be seen to be almost uniform.

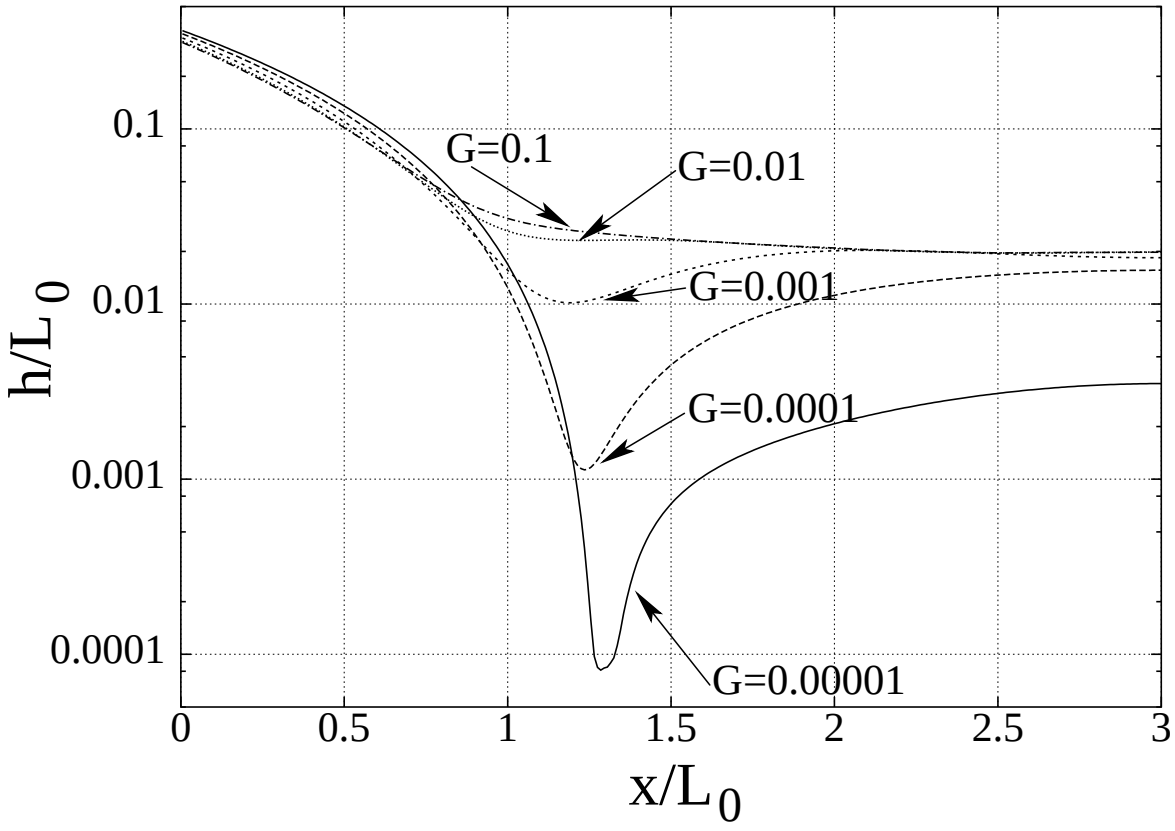

Figure 7: Final (dry) profile shapes for the parameter values given in Table I. Note that the film thickness scale is logarithmic. The surfactant strength parameter $G = K/\sigma_0$ is varied from 10^{-5} to 10^{-1}. Increasing the surfactant strength increases the final window thickness. The "dimple" is removed for G values of 0.01 or greater.

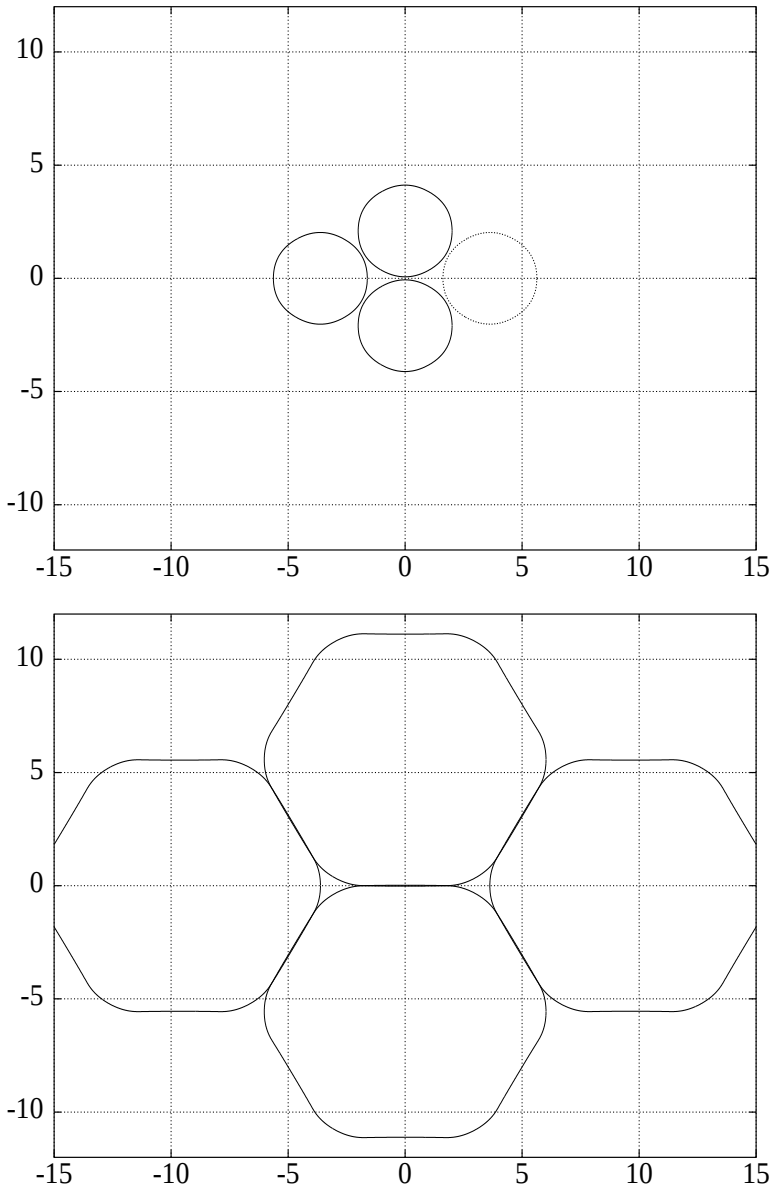

Figure 8: Four adjacent bubbles constructed from reflections and repetitions of the unit-cell shape function. Parameter values are given in Table I; G = 0.0001. Top: Initial state with gas fraction F = 0.85. Bottom: Final state of expanded foam. Two Plateau borders are seen at the interstitial corners of the almost-hexagonal bubbles. The gas fraction is now 0.978. The length unit in both pictures is L_0.

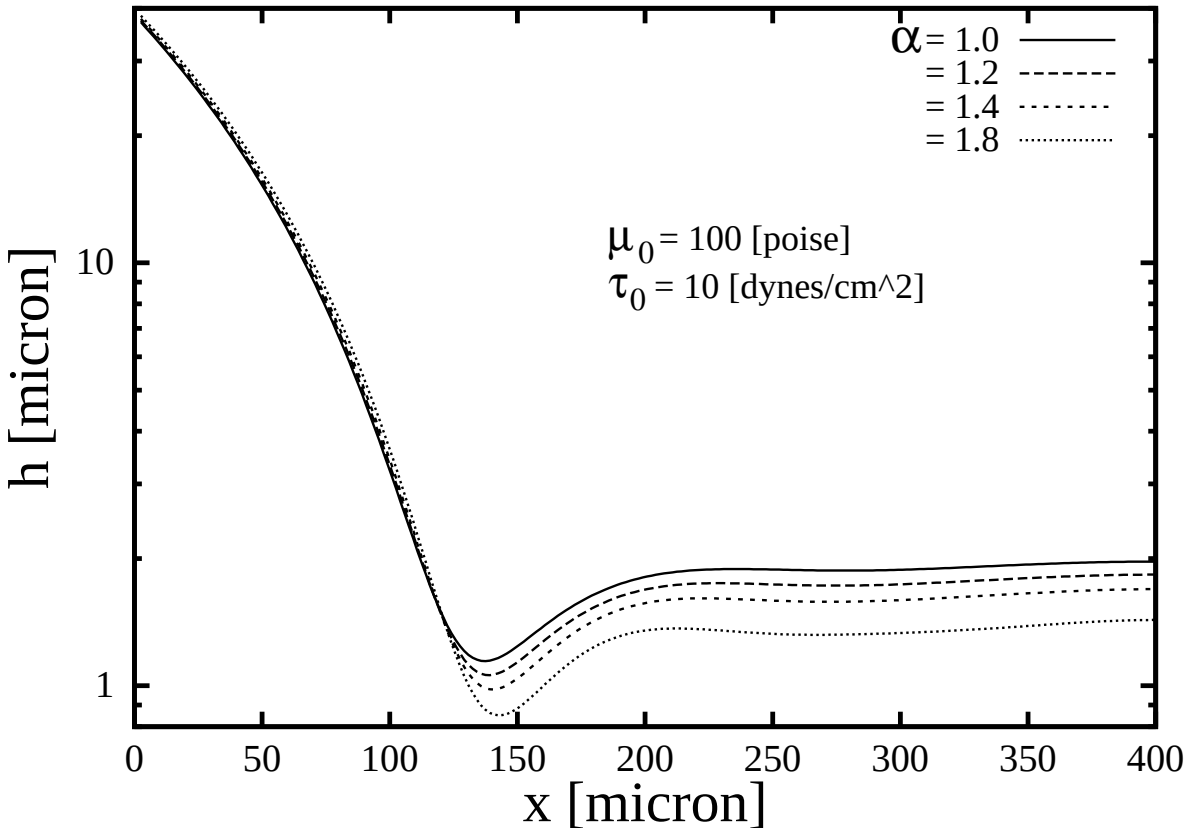

Figure 9: Final (dry) film profiles using shear and extensional thinning rheology. The modified mathematical model is given in section 8. For α = 1, the flow is Newtonian. Increasing α reduces the viscosity in those parts of the film where the stresses are large. Thinner "windows" and deeper dimples are the result of this viscosity reduction. Additional parameter values are given in the text. Note that both x and h are measured in microns here.